Progress In Electromagnetics Research C, Vol. 116, 207–219, 2021

A Novel Dual-Band Printed SIW Antenna Design Based on Fishnet & CCRR DGS Using Machine Learning for Ku-Band Applications

Mohammed F. Nakmouche[1, *], Muhammad I. Magray[2], Abdemegeed M. Allam[3], Diaa E. Fawzy[1], Ding Bing Lin[4], and Jenn-Hwen Tarng[2]

Abstract—This paper analyzes and solves the complexity to determine the optimum positions of the Fishnet & Complementary Circular Ring Resonator (CCRR) based Defected Ground Structures (DGS) for Substrate Integrated Waveguide (SIW) based antennas. A new state-of-art technique based on Artificial Neural Network (ANN)-Machine Learning (ML) is proposed for overcoming the lack of solid and standard formulations for the computation of this parameter related to a targeted frequency. As a proof of concept and to test the performance of our approach, the algorithm is applied for the determination of the CCRR and Fishnet-DGS's optimal positions for a SIW based antenna. The SIW technique provides the advantages of low cost, small size, and convenient integration with planar circuits. The ANN-ML based technique is optimized to attain dual-band resonances with optimal gain and radiation efficiency. The simulation results of the first Fishnet-DGS based antenna show good minimum return losses at two center frequencies, namely, 16.6 GHz (with gain of 6 dB and radiation efficiency of 95%) and 17.7 GHz (with gain and radiation efficiency of 9 dB and 96%, respectively). The second CCRR-DGS based antenna shows about 8 dB gain and a radiation efficiency of 87% at 17.3 GHz, and gain and efficiency of about 8.5 dB and 85% are observed at 17.8 GHz. The proposed CCRR and Fishnet-DGS based antenna are low profiles, low costs, with good gains and radiation efficiencies, making both designs very suitable for Ku-band applications. There is a fair agreement between the measured and simulated results. The achieved dual-band resonances act as a proof of concept that the proposed ANN-ML techniques can be employed for the determination of the optimal positions for CCRR and Fishnet thereby attaining any target dual-bands in the Ku-band with good accuracy of about 98% and a save of 99% in the overall the computational time.

1. INTRODUCTION

Patch antennas play an important role in the development of modern wireless communication systems due to their low profile, low cost, and simple integration with other circuit components. However, standard patch antennas have some drawbacks, for example, single frequency resonance, low impedance bandwidth, low gain, larger size, and polarization problems [1]. On the other hand, enhancements in bandwidths and gains are still topics and challenges which have attracted many researchers [2]. In [3], a dual-band patch antenna operating at 13.0 GHz and 18.1 GHz with 2.03 dB and 3.65 dB gains and radiation efficiencies of 78.4%, 82.3%, respectively, was developed. Another dual-band antenna for satellite communications with gains of about 3.37, 3.32 dB and radiation efficiencies of 81.9%, 82.5%, respectively, is presented in [4]. The low-profile patch antenna shown in [5] has an overall dimension of

Received 27 September 2021, Accepted 11 November 2021, Scheduled 20 November 2021
* Corresponding author: Mohammed F. Nakmouche (Nakmouche.MFarouk@gmail.com).
[1] Faculty of Engineering, Izmir University of Economics, Izmir, Turkey. [2] Institute of Communication Engineering, College of Electrical and Computer Engineering, National Yang Ming Chiao Tung University (NYCU), Hsinchu City, Taiwan, R.O.C.
[3] Department of Communication Engineering, German University in Cairo, Cairo, Egypt. [4] Department of Electronics and Computer Engineering, National Taiwan University of Science and Technology, Taipei, Taiwan.

$20 \times 20\,\text{mm}^2$; however, a low gain and radiation efficiency of 1.6/4.2 dB and 69%/80%, respectively, were reported. Moreover, in [6], an antenna was developed for both Ku and K frequency bands with gains of 3.1/4.13 dB and radiation efficiencies of 75.3%/86.4%, respectively. The aforementioned antennas attain low gain with low radiation efficiency.

Recently, Metamaterials (MMs) and Defected Ground Structure (DGS) have drawn the attention of researchers as approaches in the design of patch antennas and for the gain and bandwidth enhancements, as well as for the miniaturization purposes [7–13]. Metamaterials are a new class of artificially engineered materials that exhibit properties not available in nature. The properties of MMs are directly related to their unit cell structures, geometries, and sizes. This is in contrary to the conventional natural materials, where their properties are directly related to their base material composition [14]. A recently employed technique by researchers, namely DGS, shows an advantage compared to other techniques in the multiband antenna design process, keeping the antenna's overall size small with good performance [15].

Developments based on MMs and DGS-based techniques require rigorous electromagnetic (EM) simulations and lengthy computational challenges. To efficiently manage the EM numerical computational challenges and to optimize and reduce the time of the design process, ANN techniques were suggested and extensively used in antenna design process [16–21]. In [16], a mutual coupling reduction using a neural network-based technique is applied to cross-dipole antenna for base stations. Meanwhile in [17], authors used ANN to predict the optimal FSS reflector and ground's dimension for gain and bandwidth enhancement. In [18], authors used a hybrid approach based on support vector regression (SVR) and ANN to predict the size of the slots etched on the ground surface. In a work reported in [19], a hexagonal-shaped reconfigurable antenna operating at 2.36 GHz and 3.92 GHz bands was designed using ANN. In another work [20], the ANN was used to design a notch antenna loaded by an asymmetric slot. Furthermore, in [21], the ANN based optimization techniques were used to design a multiband rectangular spiral shaped microstrip antenna. However, to the best of the authors' "knowledge", few works on the application of ANN in the DGS's position for multiband antennas design are reported in literature [22, 23].

In this work, we propose a novel approach for the design of a SIW antenna based on Fishnet and Complementary Circular Ring Resonator (CCRR) MMs as DGS, with the targets of achieving dual-band resonance with good gain and efficiency using an ANN-ML based technique. Since different positions of DGS give different resonance frequencies, we used an ANN-ML algorithm to predict the optimal position of both the Fishnet and CCRR based DGS within the ground plane of the SIW cavity for a targeted resonance frequency. Section 2 presents the theoretical backgrounds of the SIW & DGS techniques and the developed ANN model. The proposed fishnet & CCRR DGS-based antenna structures with ANN modeling and simulation results are discussed in Sections 3, 4, and 5, respectively. Finally, the conclusion is given in Section 6.

2. THEORETICAL BACKGROUND

2.1. Substrate Integrated Waveguide (SIW) Technology

The SIW technology for high-frequency electronics and optoelectronics was first presented by Wu's team [24]. His work showed the advantages of the antenna to be low profile, compact in size, which in turn allows easy integration with various components (passive or active), and presents a high Q-factor and high power-handling capability. The SIW is a planar version of the classic bulky rectangular waveguide, which consists of two rows of parallel periodic via holes inserted in a dielectric substrate and connected to both the top and bottom metal layers.

As reported in [24, 25], the SIW was also used for wideband Band Pass Filter (BPF) designs, and the equivalent dimensions of the SIW as illustrated in Figure 1 are determined using the width (W) and length (L) of the classical rectangular waveguide. The diameter of the holes (d) and the spacing (p) between the holes can be determined from the following equations:

$$W_{eff} = W - 1.08 \times \left(\frac{2d}{p}\right) + 0.1 \times \left(\frac{2d}{W}\right) \tag{1}$$

$$f_{\text{TE10}} = \frac{c}{(2 \times W_{eff} \times \sqrt{\varepsilon}_r)} \tag{2}$$

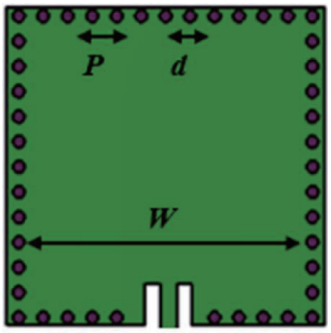

Figure 1. The SIW based parameters.

where f_{TE10} is the cut-off frequency of the dominant mode. The spacing between the two consecutive vias must be small enough to reduce the leakage loss, as given by Eq. (3) below:

$$\frac{p}{d} < 2 \tag{3}$$

2.2. Metamaterial as Defected Ground Structure (DGS)

As previously mentioned in the introduction, researchers used a simple slot structure referred to as DGS in the ground plane of the microwave planar circuits for various enhancements of the antenna parameters and size miniaturization [26–33]. The DGS consists of inductance and capacitance that creates a disturbance of the current distribution in the ground plane, which in turns creates a change in the transmission characteristics. In recent years, the use of MMs in the design of high-performance microwave components has drawn the attention of many scientists, engineers, and researchers [34].

On the other hand, MMs show properties that are directly related to their geometries and to the unit cell dimensions in comparison with conventional natural materials, where their properties are directly related to the base material composition [35]. Generally, the unit cell of the structure is smaller than the wavelength of the incident electromagnetic wave.

The use of MMs in microstrip patch antennas as a DGS affects the surface current distribution in the ground plane and leads to the creation of second resonance frequency. Different positions of DGS give different resonance frequencies. The Fishnet and CCSR MMs structures are popular and commonly used structures. For the current work, we use ANN-ML algorithm to predict the optimal positions of both the Fishnet and CCRR based DGS within the ground plane of the SIW cavity for a targeted resonance frequency with enhanced gain and fractional bandwidth for Ku-band applications (radar and satellite communications). The geometries of the two-unit cells are illustrated in Figure 2, and the design parameters are presented in Table 1.

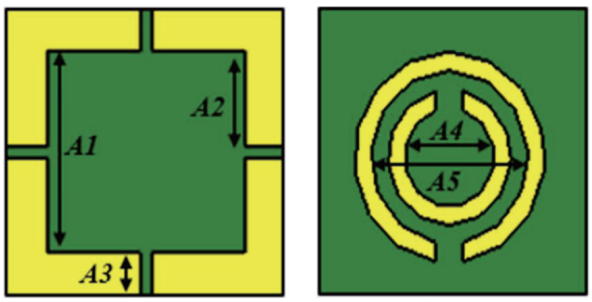

Figure 2. The geometry of the proposed DGS's unit cells. (a) Fishnet-DGS unit cell. (b) CCRR-DGS unit cell.

Table 1. The design parameters of the unit cells.

Variables	A1	A2	A3
Value (mm)	3.50	1.75	1.75
Variables	A4	A5	A6
Value (mm)	0.75	2.60	4.60

2.3. Machine Learning

The ANN is used to predict the optimal positions of both the Fishnet and CCSR based DGS within the ground plane of the SIW cavity in terms of the resonance frequency. The input parameters of the developed ANN model are the two-resonance frequency and Fishnet/CCSR-DGS X & Y positions as output, together with a hidden layer of 100 neurons (the number of neurons is chosen based on the regression output where 10 neurons present accurate results as shown in Table 2).

Table 2. Regression values for different numbers of neurons.

Number of neurons	5	10	25	50	75	100
Regression outputs (R)	0.13	0.95	0.88	0.77	0.61	0.42

Figure 3 shows the developed model. As reported in Table 3, the back propagation along with Levenberg-Marquart (LM) learning algorithm is chosen with a learning rate of 0.09, which is the developed ANN model adaptation rate to the problem with epochs number of 100, which indicates the number of times that the ANN model operates through the entire training dataset.

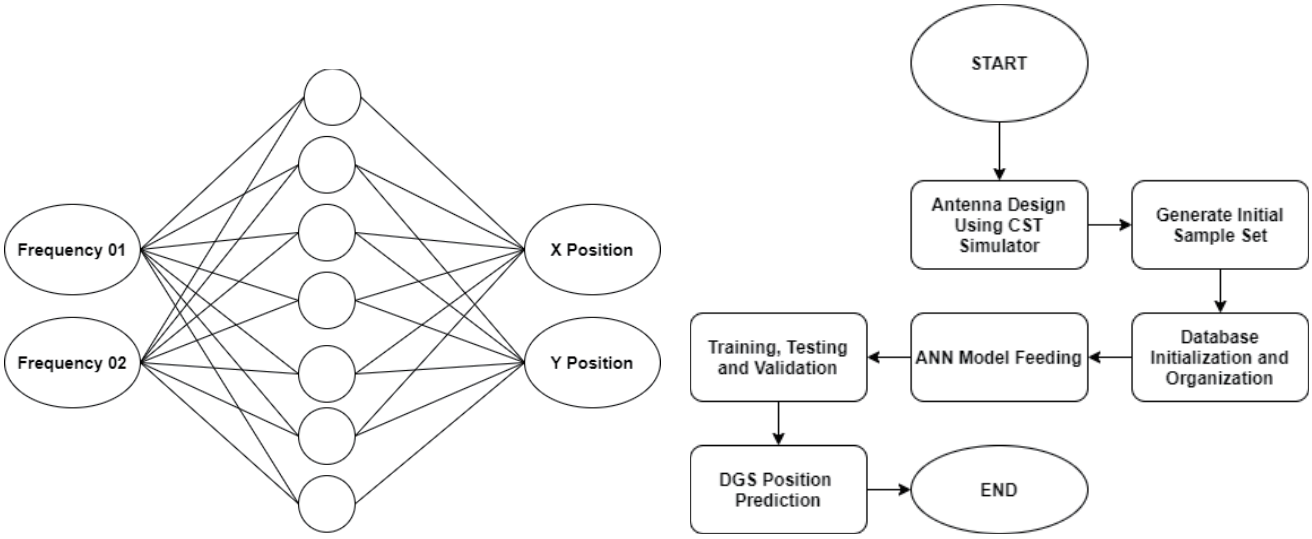

(a) (b)

Figure 3. The proposed ANN-ML approach. (a) ANN-ML Model. (b) ANN-ML Flow chart.

3. ANTENNA DESIGN

This section describes the designs of the Fishnet/CCSR-DGS based antennas. The initial patch length and width are computed based on the standard well-known basic equations for patch antenna design

Table 3. The main parameters of the developed ann model.

Antenna Parameters	Parameters Value
Neurons in Input Layer	2
Neurons in Output Layer	4
Neurons in Hidden Layer	10
Learning Rate	0.09
Number of Epochs	100
Training Algorithm	Levengberg-Marquardt (LM)

as reported in [36]. Figure 4(a) shows the proposed antenna with its outlined dimensions depicted in Table 4. Equations (1)–(3) are used to develop the SIW structure. The proposed antennas are designed on 1.6 mm thick Roger5058 material with relative permittivity (ε_r) of 2.2 and loss tangent of 0.0009.

Concerning the fishnet-DGS-based antenna, the bottom view configuration with 12 fishnet unit cells as 4×3 array etched in the ground plane is shown Figure 4(b). The bottom view of CCRR-DGS based antenna structure is illustrated in Figure 4(c) with an array of 3×3 and 6 CCRR unit cells slotted in the ground plane. The proposed antenna's overall dimension is $65 \times 56\,\text{mm}^2$ with a 50-Ω microstrip fed line of $5.7 \times 27\,\text{mm}^2$ optimized for good impedance matching.

The fabricated versions of both antennas are depicted in Figure 5. The optimization of the initial values using CST EM simulator software is conducted to match the required initial responses.

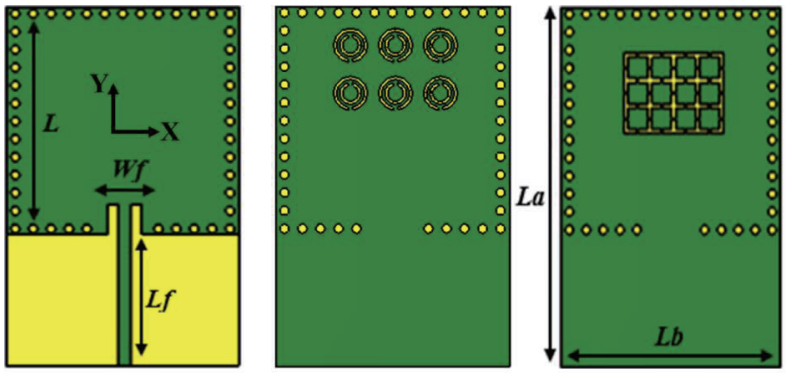

Figure 4. Proposed antennas. (a) Antenna top view. (b) Bottom view of the Fishnet-DGS based antenna. (c) Bottom view of CCRR-DGS based antenna.

Table 4. Design parameters of the proposed antennas.

Variables	La	Lb	L
Value (mm)	60	39	38
Variables	Lf	Lg	Wg
Value (mm)	27	5	5.7

4. ANN MODELING

Using CST EM simulator software, the overall simulation for different Fishnet/CCSR-DGS positions in terms of resonance frequencies and reflection coefficients is first conducted. Then, the CST output

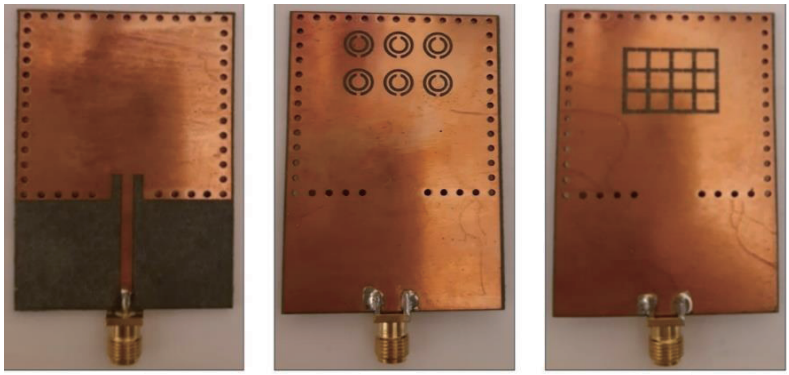

Figure 5. Fabricated antennas. (a) Top view of the proposed antenna. (b) Bottom view of the CCRR DGS based antenna. (c) Bottom of the Fishnet DGS based antenna.

results are organized as a dataset and fed into the ANN model. 75% of the datasets are used to train the ANN model, 10% for validation, and 15% for testing. Lastly, the optimal Fishnet/CCSR-DGS position is extracted using the trained ANN. Figure 7 illustrates the reflection coefficient for different Fishnet/CCSR-DGS positions. It is found that the optimum position is at the centre (Xopt = 0 and Yopt = 0).

In order to validate the proposed ANN model, a comparison between the CST and ANN results in terms of resonant frequency and reflection coefficients is conducted and reported in Tables 5, 6, 7, and 8. Furthermore, the mean square errors are also depicted in Table 9 and Table 10. It can be noticed that the CST and predicted ANN results are very close.

With the aim to analyze the developed ANN over-fitting characteristics, the R-value (Related to training, validation and testing) is calculated. An R-value close to 1 means that the proposed ANN model learning and training is conducted perfectly, while an R-value far from 1 means that we have an over-fitting and by that the ANN model cannot generalize new test data, and it just memorizes the historic training set. The proposed ANN results show a regression output (R) value of ≈ 0.91 for the Fishnet-DGS based antenna case and ≈ 0.92 for the CCRR-DGS based antenna case as shown in Figure 6.

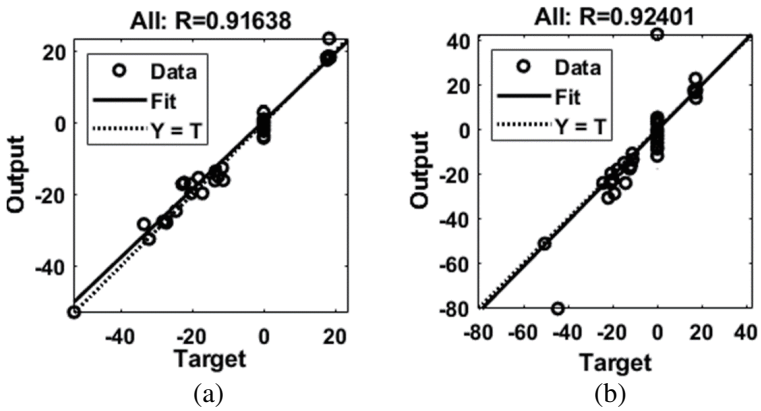

Figure 6. ANN regression outputs (R) for all training, validation and testing to Fishnet-DGS & CCRR-DGS based antenna. (a) Fishnet-DGS based antenna. (b) CCRR-DGS based antenna.

Table 5. A comparison between the CST and predicted ANN resonant frequencies for different Xpos/Ypos values for the fishnet DGS based antenna.

		Input		Targets (Simulated by CST)		Outputs (Estimated by ANN)	
		Xopt Position	Yopt Position	Freq 01 (GHz)	Freq 02 (GHz)	Freq 01 (GHz)	Freq 02 (GHz)
Training Data	**01**	0	−1	17.82	NA	17.80	NA
	02	0	−7	17.67	NA	17.65	NA
	...	...	...	...	...	...	...
	...	...	...	...	...	...	...
	74	2	2	16.125	17.75	16.128	17.76
	75	2	−1	17.75	NA	17.76	NA
Validation Data	**76**	3	−7	18.60	NA	18.61	NA
	77	4	−1	17.125	NA	17.13	NA
	...	...	...	...	...	...	...
	...	...	...	...	...	...	...
	89	4	−10	16.9	NA	16.88	NA
	90	−1	2	16.9	17.2	16.89	17.21
Testing Data	**91**	−2	2	17.88	18.30	17.87	18.32
	92	−4	2	17.82	18.21	17.81	18.22
	...	...	...	...	...	...	...
	...	...	...	...	...	...	...
	99	0	0	16.6	17.7	16.598	17.705
	100	−4	−1	17.85	NA	17.84	NA

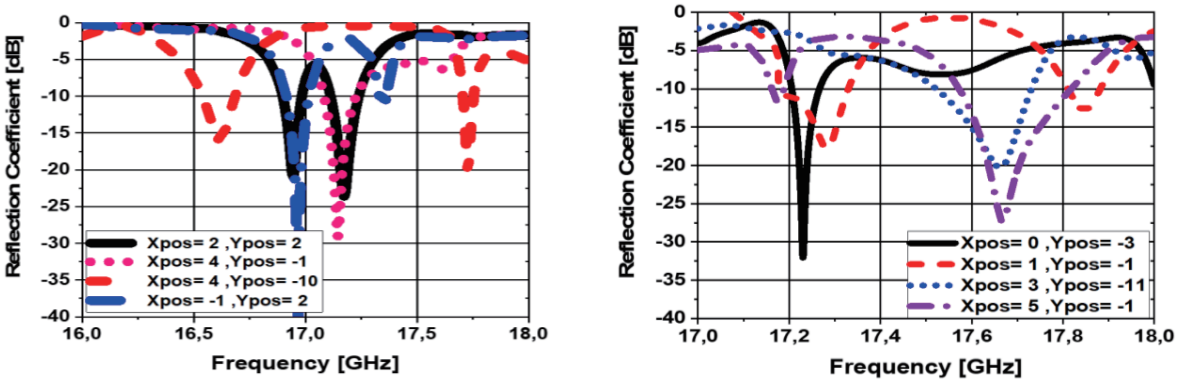

(a) (b)

Figure 7. Reflection coefficients for different Fishnet/CCRR-DGS positions. (a) Fishnet-DGS based antenna. (b) CCRR-DGS based antenna.

5. RESULTS AND DISCUSSIONS

5.1. Proposed Fishnet-DGS Based Antenna Results

Figure 8 illustrates the simulated and measured return losses of the fishnet-based antenna. It is observed that the proposed antenna with fishnet MMs operates at both frequencies of 16.6 GHz and 17.7 GHz with acceptable return losses. The gain and directivity usually show the efficiency of the antenna and

Table 6. A comparison between the CST and predicted ANN resonant frequencies for different Xpos/Ypos values for the CCSR antenna.

		Input		Targets (Simulated by CST)		Outputs (Estimated by ANN)	
		Xopt Position	Yopt Position	Freq 01 (GHz)	Freq 02 (GHz)	Freq 01 (GHz)	Freq 02 (GHz)
Training Data	**01**	0	−1	17.34	16.96	17.338	16.95
	02	0	−3	17.3	18.85	17.29	18.86
	...	...	...	...	...	...	...
	...	...	...	...	...	...	...
	74	1	−1	17.15	17.65	17.12	17.63
	75	2	−5	16.86	NA	16.859	NA
Validation Data	**76**	3	−11	17.25	NA	17.23	NA
	77	5	−1	17.65	NA	17.64	NA
	...	...	...	...	...	...	...
	...	...	...	...	...	...	...
	89	4	−7	17.02	NA	17.02	NA
	90	3	−11	16.98	NA	16.98	NA
Testing Data	**91**	5	−3	17.25	NA	17.25	NA
	92	−1	−1	16.90	17.17	16.90	17.17
	...	...	...	...	...	...	...
	...	...	...	...	...	...	...
	99	0	0	17.3	17.8	17.29	17.79
	100	−4	−3	17.26	NA	17.26	NA

Table 7. Mean square errors for fishnet & CCSR-DGS based antenna.

Design Parameters	Mean Square Error (MSE)			
	Fishnet DGS Antenna		CCSR DGS Antenna	
	Freq 01 (GHz)	Freq 02 (GHz)	Freq 01 (GHz)	Freq 02 (GHz)
Optimal X & Y Position	1.53×10^{-04}	6.04×10^{-05}	1.33×10^{-04}	5.03×10^{-05}

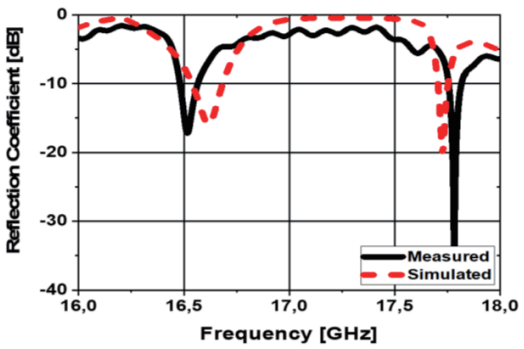

Figure 8. Simulated and measured S_{11} values of the proposed antenna with fishnet unit cell.

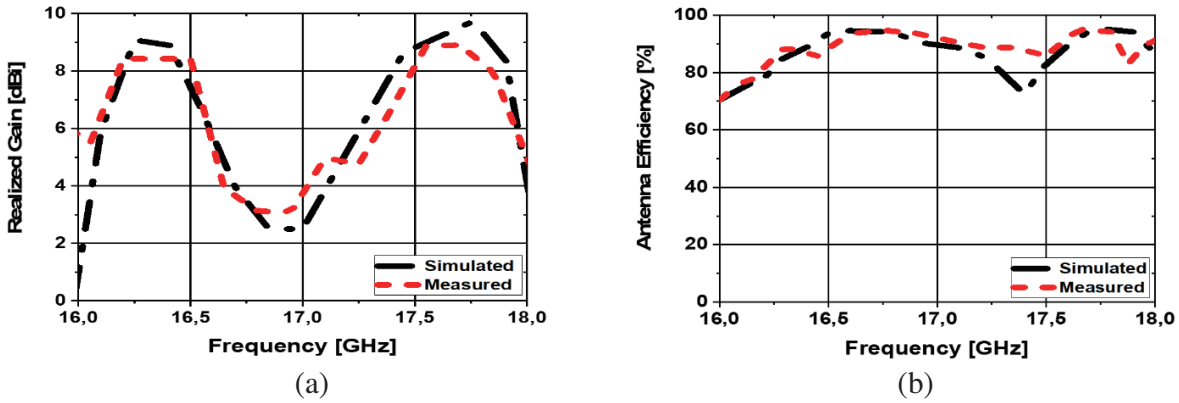

(a) (b)

Figure 9. Simulated & measured gain & efficiency of the proposed antenna with H-slotted DGS. (a) Gain. (b) Efficiency.

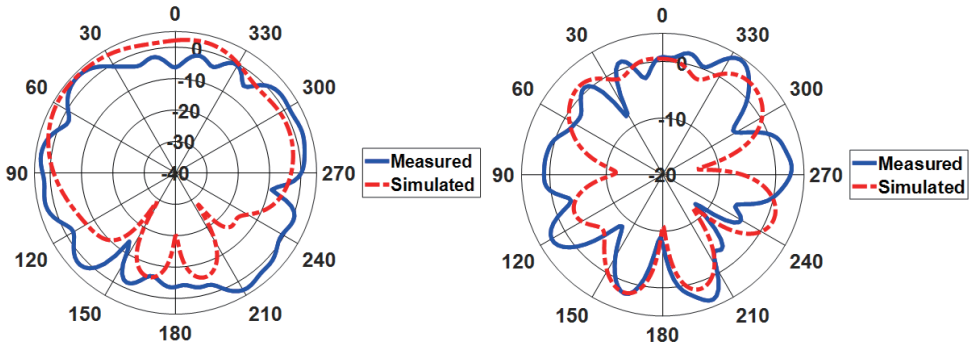

(a) (b)

Figure 10. Simulated and measured radiation patterns of the antenna with fishnet unit cell in E-plane at (a) 16.6 GHz and (b) 17.7 GHz.

its directional capabilities, and for the current design, the obtained gains are 6 dB and 9 dB at 16.6 GHz and 17.7 GHz, respectively as shown in Figure 9(a). On the other hand, there is a fair agreement between the measured and simulated return losses of the antenna. The antenna's efficiencies are 95% and 96% at 16.6 GHz and 17.7 GHz, respectively as illustrated in Figure 9(b). The plots of the radiation patterns in E-plane (YZ-plane) are presented in Figure 10 for the frequencies 16.6 GHz and 17.7 GHz. The proposed antenna achieves broadside radiation patterns with high front-to-back ratio.

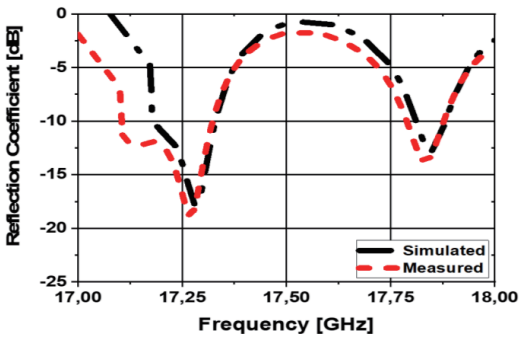

Figure 11. Simulated S_{11} of the proposed antenna with CCRR unit cell.

5.2. Proposed CCRR-DGS Based Antenna Results

A dual-band antenna is designed and analysed based on CCRR-DGS. The simulated and measured S_{11} results are plotted in Figure 11. The proposed antenna operates at two resonance frequencies, 17.3 GHz and 17.8 GHz, respectively. The obtained measurements show good matching between the simulated and measured results.

The antenna gain is 8 dB at 17.3 GHz band frequency. At 17.8 GHz band frequency, we notice a gain of 8.5 dB with radiation efficiencies of 87% and 85% at both resonance frequencies as shown in Figure 12. The radiation patterns in E-plane (YZ-plane) are shown in Figures 13. Radiation patterns are uniform and stable in nature with high front-to-back ratio.

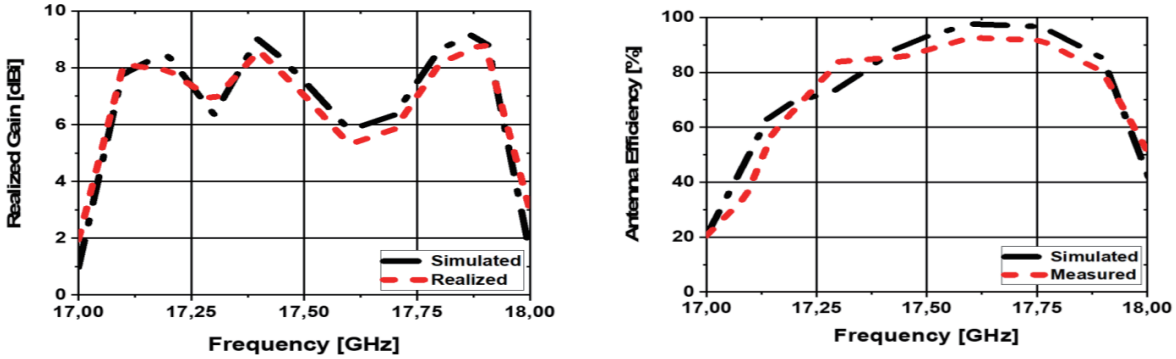

(a) (b)

Figure 12. Simulated & measured gain & efficiency of the proposed antenna with H-slotted DGS. (a) Gain. (b) Efficiency.

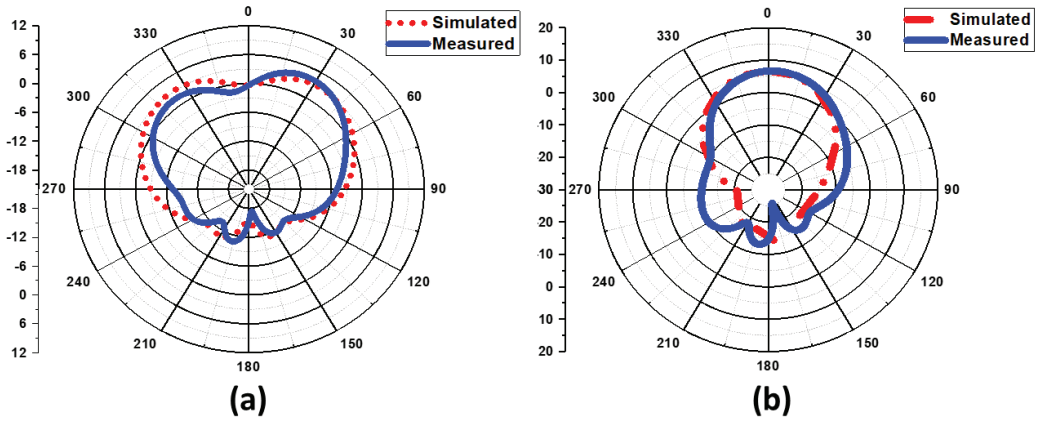

Figure 13. Simulated and measured radiation patterns of the antenna with CCRR unit cell in E-plane at (a) 17.3 GHz and (b) 17.8 GHz.

Due to the SMA connectors and the environment in which the measurements are conducted, a noise and some mismatching between simulation and measurement results can be noticed but can still be neglected and acceptable as an experimental validation since the other parameters such as reflection coefficient, realized gain, and radiation efficiency are quite stable.

A comparison between the two proposed antennas and similar studies published in the literature is presented in Table 8. Based on the three main parameters: the operating frequency, gain, and antenna efficiency, one can notice that the fishnet-based and CCRR-based antennas have better gain and efficiency in comparison with other studies.

Table 8. Comparison of the proposed antenna with previous work.

Comparison Parameter	Operating Frequency (GHz)	Gain (dB)	Radiation Efficiency
[3]	13.0 18.1	2.03 3.65	78.4% 82.3%
[4]	15.15 18.2	3.37 3.32	81.9% 82.5%
[5]	12.38 14.40	1.6 4.2	69% 80%
[6]	12.94 19.04	3.1 4.13	75.3% 86.4%
[37]	9.85 14	6.62 6.44	Not Mentioned
[38]	9.55 10.35	6 6.6	Not Mentioned
Fishnet Based Antenna	16.6 17.7	≈ 8	$> 95\%$
CCRR Based antenna	17.3 17.8	≈ 7.5 ≈ 8	$> 80\%$

6. CONCLUSION

A new state-of-art technique based on ANN-ML technique is proposed for overcoming the lack of solid and standard formulations for the computation of DGS position in terms of a targeted resonances frequency. As a proof of concept and to test the performance of our approach, the algorithm is applied for the determination of the CCRR and Fishnet-DGS's optimal positions in terms of a targeted resonance frequency for Ku-band applications such as radar and satellite communication.

The performance of proposed Fishnet-DGS based antenna shows a dual band response with good enhancement in gain and in its radiation efficiencies as well. The proposed fishnet-DGS based antenna resonates at center frequencies of 17.87 GHz (with a gain of 4.74 dB) and 18.38 GHz (with a gain of 5.95 dB is observed). Meanwhile, the CCRR-DGS based antenna's gain is 6.49 dB at 16.91 GHz center frequency, and at 17.32 GHz center frequency, a gain of 7.55 dB is noticed. Both configurations show a high radiation efficiency of about 90%. There is a fair agreement between the measured and simulated results which act as a proof of concept that the proposed ANN-ML techniques can be employed for the determination of the optimal positions for CCRR and Fishnet thereby attaining any target dual-bands in the Ku-band with good accuracy of about 98% and a save of 99% in the overall computational time.

REFERENCES

1. Madhav, B. T. P., M. Manjeera, M. S. Navya, D. S. Devi, and V. Sumanth, "Novel metamaterial loaded multiband patch antenna," *Indian J. Sci. Technol.*, Vol. 9, No. 38, 2016.
2. Khandelwal, M. K., B. K. Kanaujia, and S. Kumar, "Defected ground structure: Fundamentals, analysis, and applications in modern wireless trends," *Int. J. Antennas Propag.*, Vol. 2017, 2017.
3. Ahsan, M. R., M. T. Islam, M. H. Ullah, R. W. Aldhaheri, and M. M. Sheikh, "A new design approach for dual-band patch antenna serving Ku/K band satellite communications," *Int. J. Satell. Commun. Network*, Vol. 34, 759–769, 2016.

4. Ullah, M. H., M. T. Islam, M. R. Ahsan, J. S. Mandeep, and N. Misran, "A dual band slotted patch antenna on dielectric material substrate," *Int. J. Antennas Propag.*, Vol. 2014, 2014.
5. Saini, G. S. and R. Kumar, "A low profile patch antenna for Ku-band applications," *Int. J. Electron. Lett.*, Vol. 00, No. 00, 1–11, 2019.
6. Ahsan, M. R., M. T. Islam, and M. H. Ullah, "A simple design of planar microstrip antenna on composite material substrate for Ku/K band satellite applications," *Int. J. Commun. Syst.*, Vol. 30, e2970, 2017.
7. Da Silva, I. B. T., H. D. de Andrade, J. L. da Silva, H. C. C. Fernandes, and J. P. P. Pereira, "Design of microstrip patch antenna with complementary split ring resonator device for wideband systems application," *Microw. Opt. Technol. Lett.*, Vol. 57, 1326–1330, 2015.
8. Nakmouche, M. F., D. E. Fawzy, A. M. M. A. Allam, H. Taher, and M. F. A. Sree, "Dual band SIW patch antenna based on H-slotted DGS for Ku band application," *2020 7th Int. Conf. Electr. Electron. Eng. ICEEE 2020*, 194–197, 2020.
9. Roy, S. and U. Chakraborty, "Metamaterial-embedded dual wideband microstrip antenna for 2.4 GHz WLAN and 8.2 GHz ITU band applications," *Waves in Random and Complex Media*, Vol. 30, No. 2, 193–207, 2020.
10. Zhang, H. T., G. Q. Luo, B. Yuan, and X. H. Zhang, "A novel ultra-wideband metamaterial antenna using chessboard-shaped patch," *Microw. Opt. Technol. Lett.*, Vol. 58, 3008–3012, 2016.
11. Rajak, N., N. Chattoraj, and R. Mark, "Metamaterial cell inspired high gain multiband antenna for wireless applications," *AEU — Int. J. Electron. Commun.*, Vol. 109, 23–30, 2019.
12. Singh, A. K., M. P. Abegaonkar, and S. K. Koul, "Miniaturized multiband microstrip patch antenna using metamaterial loading for wireless application," *Progress In Electromagnetics Research C*, Vol. 83, 71–82, 2018.
13. Kumar, P., T. Ali, and M. M. M. Pai, "Electromagnetic metamaterials: A new paradigm of antenna design," *IEEE Access*, Vol. 9, 2021.
14. Shelby, R. A., D. R. Smith, S. C. Nemat-Nasser, and S. Schultz, "Microwave transmission through a two-dimensional, isotropic, left-handed metamaterial," *Appl. Phys. Lett.*, Vol. 78, No. 4, 489–491, 2001.
15. Liu, Y., X. Yang, Y. Jia, and Y. J. Guo, "A low correlation and mutual coupling MIMO antenna," *IEEE Access*, Vol. 7, 127384–127392, 2019.
16. Ozdemir, E., O. Akgol, F. O. Alkurt, M. Karaaslan, Y. I. Abdulkarim, and L. Deng, "Mutual coupling reduction of cross-dipole antenna for base stations by using a neural network approach," *Appl. Sci.*, Vol. 10, No. 1, 2020.
17. Nakmouche, M. F., A. M. Allam, D. E. Fawzy, and D.-B. Lin, "Development of a high gain fss reflector backed monopole antenna using machine learning for 5G applications," *Progress In Electromagnetics Research M*, Vol. 105, 183–194, 2021.
18. Khan, T. and C. Roy, "Prediction of slot-position and slot-size of a microstrip antenna using support vector regression," *Int. J. RF Microw Comput. Aided Eng.*, 2019.
19. Kumar, R., P. Kumar, S. Singh, and R. Vijay, "Fast and accurate synthesis of frequency reconfigurable slot antenna using back propagation network," *AEU — Int. J. Electron. Commun.*, Vol. 112, 152962, 2019.
20. Sabanci, K., A. Kayabasi, A. Toktas, and E. Yigit, "Notch antenna analysis: Artificial neural network-based operating frequency estimator," *Appl. Comput. Electromagn. Soc. J.*, Vol. 32, No. 4, 303–309, 2017.
21. Aoad, A., "Design and manufacture of a multiband rectangular spiral-shaped microstrip antenna using EM-driven and machine learning," *Elektron. ir Elektrotechnika*, Vol. 27, No. 1, 29–40, 2021.
22. Nakmouche, M. F., A. M. M. A. Allam, D. E. Fawzy, D. B. Lin, M. Fathy, and A. Sree, "Development of H-slotted DGS based dual band antenna using ANN for 5G applications," *15th Eur. Conf. Antennas Propag. (EuCap)*, 2021.
23. Nakmouche, M. F., A. M. M. A. Allam, D. E. Fawzy, and D. B. Lin, "Low profile dual band H-slotted DGS based antenna design using ANN for K/Ku band applications," *2021 8th Int. Conf.*

Electr. Electron. Eng. ICEEE, 2021.

24. Bozzi, M., A. Georgiadis, and K. Wu, "Review of substrate-integrated waveguide circuits and antennas," *IET Microwaves, Antennas Propag.*, Vol. 5, No. 8, 909–920, 2011.
25. Nakmouche, M. F., H. Taher, D. E. Fawzy, and G. Kahraman, "Parametric study of different shapes-slotted substrate integrated waveguide for wideband applications," *Mediterr. Microw. Symp.*, 251–254, 2019.
26. Nakmouche, M. F., H. Taher, D. E. Fawzy, and A. M. M. A. Allam, "Development of a wideband substrate integrated waveguide bandpass filter using H-slotted DGS," *in Proceedings — CAMA 2019: IEEE International Conference on Antenna Measurements and Applications*, 2019.
27. Feng, S., L. Zhang, H. W. Yu, Y. X. Zhang, and Y. C. Jiao, "A single-layer wideband differential-fed microstrip patch antenna with complementary split-ring resonators loaded," *IEEE Access*, Vol. 7, 132041–132048, 2019.
28. Tao, L., et al., "Bandwidth enhancement of microstrip patch antenna using complementary rhombus resonator," *Wirel. Commun. Mob. Comput.*, Vol. 2018, 2018.
29. Jilani, S. F. and A. Alomainy, "Millimetre-wave T-shaped MIMO antenna with defected ground structures for 5G cellular networks," *IET Microwaves, Antennas Propag.*, Vol. 12, No. 5, 672–677, 2018.
30. Patel, R., A. Desai, T. Upadhyaya, T. K. Nguyen, H. Kaushal, and V. Dhasarathan, "Meandered low profile multiband antenna for wireless communication applications," *Wirel. Networks*, Vol. 27, No. 1, 1–12, 2021.
31. Gopi, D., A. R. Vadaboyina, and J. R. K. K. Dabbakuti, "DGS based monopole circular-shaped patch antenna for UWB applications," *SN Appl. Sci.*, Vol. 3, No. 2, 2021.
32. Salih, A. A. and M. S. Sharawi, "A dual-band highly miniaturized patch antenna," *IEEE Antennas Wirel. Propag. Lett.*, Vol. 15, No. 12, 1783–1786, 2016.
33. Xu, Z., Q. Zhang, and L. Guo, "A compact 5G decoupling MIMO antenna based on split-ring resonators," *Int. J. Antennas Propag.*, Vol. 2019, 2019.
34. Nakmouche, M. F. and M. Nassim, "Impact of metamaterials DGS in PIFA antennas for IoT terminals design," *in Proceedings — 2019 6th International Conference on Image and Signal Processing and their Applications, ISPA 2019*, 2019.
35. Kumar, A., R. Patel, and M. V. Kartikeyan, "Investigation on microstrip filters with CSRR defected ground structure," *Adv. Electromagn.*, Vol. 5, No. 2, 28–33, 2016.
36. Balanis, C. A., *Antenna Theory Analysis and Design*, 3rd Edition, 2005.
37. Lokeshwar, B., D. Venkatasekhar, and A. Sudhakar, "Dual-band low profile siw cavity-backed antenna by using bilateral slots," *Progress In Electromagnetics Research C*, Vol. 100, 263–273, 2020.
38. Lokeshwar, B., D. Venkatasekhar, and J. Ravindranadh, "Development of a low-profile broadband cavity backed bow-tie shaped slot antenna in SIW technology," *Progress In Electromagnetics Research Letters*, Vol. 100, 9–17, 2021.